

# A PRELIMINARY FEASIBILITY STUDY ON MULTI-CAVITY CRYOMODULE INTEGRATION FOR THE ELECTRON ION COLLIDER ENERGY RECOVER LINAC COOLER

S. Setiniyaz<sup>1\*</sup>, S. Benson<sup>1</sup>, I. Neththikumara<sup>1</sup>, K. Deitrick<sup>1</sup>, C. Gulliford<sup>2</sup>, J. Guo<sup>1</sup>,  
C. Mayes<sup>2</sup>, T. Satogata<sup>1</sup>, N. Sereno<sup>1</sup> and N. Taylor<sup>2</sup>

<sup>1</sup>Thomas Jefferson National Accelerator Facility, Newport News, VA, USA

<sup>2</sup>Xelera Research LLC, Ithaca, NY, USA

## Abstract

The Electron-Ion Collider (EIC) is a state-of-the-art accelerator designed for collisions between highly polarized electrons and ions. To achieve optimal luminosity, the ion beam is cooled using an electron beam sourced from an energy recovery linac (ERL). In the current ERL baseline design, one BNL type RF cavity is used per cryomodule, leading to spatial and cost challenges. This study examines the feasibility of using more compact PERLE (Powerful Energy Recovery Linac for Experiments) type cavities, which can house multiple cavities within a single cryomodule, by evaluating their Beam Breakup (BBU) instability performance. Higher Order Modes (HOM) parameters were obtained through frequency scaling, assuming constant quality factor  $Q_L$ , R/Q, and linearly scaling HOM frequencies. To predict the BBU threshold current and ensure accuracy, two different BBU tracking simulations are used for cross-verification. Although the reduced footprint of PERLE-type cavities is advantageous, maintaining sufficient damping of HOMs remains crucial. Finally, we compare the HOM damping efficiency of both cavity types and suggest a pathway forward.

## INTRODUCTION

The Electron-Ion Collider (EIC) is a new high luminosity particle accelerator designed to collide highly polarized electrons and ions [1,2]. Planned for construction at Brookhaven National Laboratory (BNL) in collaboration with Thomas Jefferson Laboratory (JLab), the EIC aims to achieve its high luminosity through a novel Coherent electron Cooling (CeC) method [3]. The electron beam of the CeC is delivered by an high current Energy Recovery Linac (ERL) [4]. The ERL-based cooler in principle can recover the electron beam energy after cooling, thus saves energy cost. The layout of the EIC and ERL is shown in the Fig. 1 [5].

The ERL Cooler's design specifications are listed in Table 1. For CeC cooling, it requires 1 nC bunch charges and a 98.5 MHz repetition rate, resulting in a current of 98.5 mA. The ERL can operate in two energy modes: mode-A at 150 MeV (used for cooling 275 GeV beams) and mode-B at 55 MeV (used for cooling 100 GeV beams). The beam has a flat-top super-Gaussian longitudinal distribution with an order of 2.6 and RMS bunch length provided in the table.

\* saitiniy@jlab.org

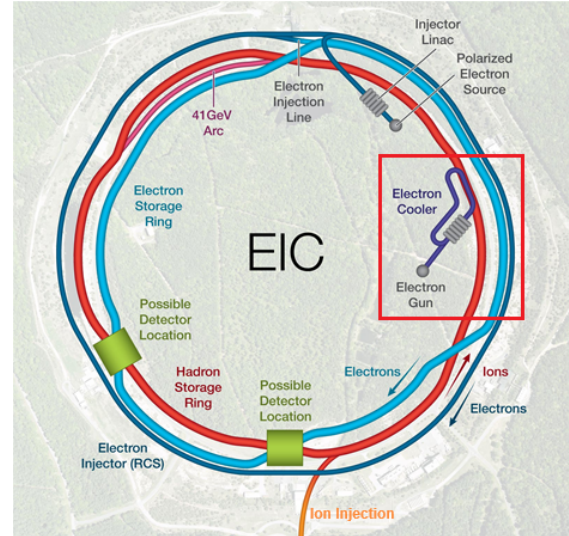


Figure 1: Schematic Layout of the Electron-Ion Collider (EIC) and Energy Recovery Linac (ERL) Cooler [5].

Table 1: ERL Cooler Electron Beam Specifications

Parameters	Mode-B	Mode-A
nominal energy (MeV)	55	150
normalized emittance (mm-mrad)	2.8	2.8
repetition rate (MHz)	98.5	98.5
bunch charge (nC)	1	1
beam current (mA)	98.5	98.5
RMS bunch length (mm)	9	7

Figure 2 shows a simplified layout of the ERL Cooler beamline. Note that some elements are not drawn to scale for better clarity. The initial electron beam is accelerated up to 6 MeV by two 197 MHz cavities and then injected into the recirculating section of the ERL. The injected beam passes through a series of 197, 591, and 1773 MHz cavities and is accelerated up 55 MeV in mode-B. Following acceleration, the electron beam is injected into the modulator section of the hadron ring, where it co-propagates with the hadron beam. This section is followed by an amplifier, a kicker, and finally a return path to the cavities. The electron beam then enters the cavities in a deceleration phase to recover its energy. For a more detailed description of the beamline design, please refer to Ref. [7].

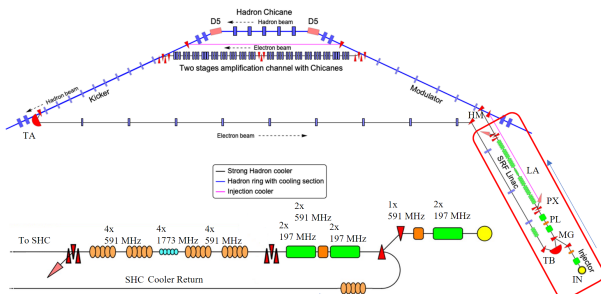


Figure 2: Representative layout of ERL Cooler.

The current baseline design of the ERL Cooler uses a 650 MHz 5-cell BNL type cavity [8, 9] and frequency scales it for the 5-cell 197, 591, and 1773 MHz frequencies. However, a drawback of the BNL-type cavity is its single-cavity-per-cryomodule configuration, which requires a lot of space. This work aims to explore the possibility of adopting a more compact 5-cell 802 MHz PERLE (Powerful Energy Recovery Linac for Experiments) cavity design [10, 11], which accommodates up to four cavities per cryomodule, reducing both spatial requirements and costs.

## HIGHER ORDER MODES

When the beam passes through the cavities, it interacts with them and induces electromagnetic fields that remain trapped inside, known as wake fields. Wake fields at certain resonant frequencies and below a cutoff frequency can persist within the cavities for a significant duration, affecting subsequent bunches. These are referred to as long-range wake fields and trapped modes. The cutoff frequency is inversely proportional to the cavity iris size. Monopole modes have longitudinal wake fields that can lead to energy and timing jitters in the beam. However, their impact on beam instabilities is minimal and can be mitigated through appropriate off-crest acceleration/deceleration. In contrast, dipole modes produce transverse wake fields that can deflect the beam, causing transverse BBU instabilities. This study specifically focuses on the dipole HOMs and transverse BBU instability, as they are more dominant.

To estimate BBU instabilities, it's essential to have HOM parameters obtained through direct measurements or simulations. At this early stage of the project, we don't have detailed technical designs of the cavities at the required frequencies. Therefore, Higher Order Modes (HOM) parameters are derived using the frequency scaling method [12], where the loaded quality factor  $Q_L$  and transverse shunt impedance  $(\frac{R}{Q})_{\perp}$  remain constant, while HOM frequencies  $f$  scale linearly. The figure of merit  $\xi$  used to estimate the dominance of dipole modes is given as [13]

$$\xi = \frac{\frac{k^2}{2} \left( \frac{R}{Q} \right)_{\perp} \sqrt{Q_L}}{f} \quad (1)$$

with  $k$  representing of the wave number of the HOM in question. The higher the value of  $\xi$ , the more dominant the mode.

Figure 3 compares the frequency-scaled figures of merit for the BNL and PERLE types of cavities at three different frequencies for the 30 most dominant dipole HOMs. The data reveals that the most dominant modes of the PERLE cavity have significantly higher  $\xi$  values compared to those of the BNL cavity. Since BBU instabilities and threshold currents are primarily influenced by the one or two most dominant modes, BNL-type cavities are anticipated to be more stable and generate higher threshold currents. Additionally, the dominant modes originate from the 1773 MHz cavities, suggesting these are likely to be the most unstable and set the threshold.

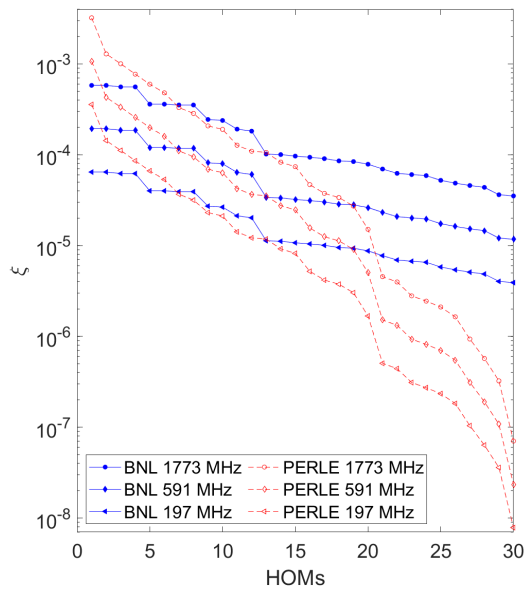


Figure 3: Comparison of figure of merits for BNL and PERLE type cavities after frequency scaling. The modes are ranked from the highest to the lowest  $\xi$ .

## BBU SIMULATION

BBU tracking simulations were carried out using two different tracking programs: Bmad BBU [14] and a MATLAB-based BBU tracking code developed in-house. Both programs estimate BBU instabilities and threshold currents by tracking particles through cavities where HOM voltages are excited and where particles receive kicks from HOMs excited by previous bunches. In both codes, a single macro particle represents the entire bunch, and the transfer matrices of the beamline elements between cavities are combined to accelerate the simulation. We focus specifically on simulations of mode B due to its lower beam energy, making it more susceptible to BBU instabilities, as low-energy bunches are more significantly affected by kicks.

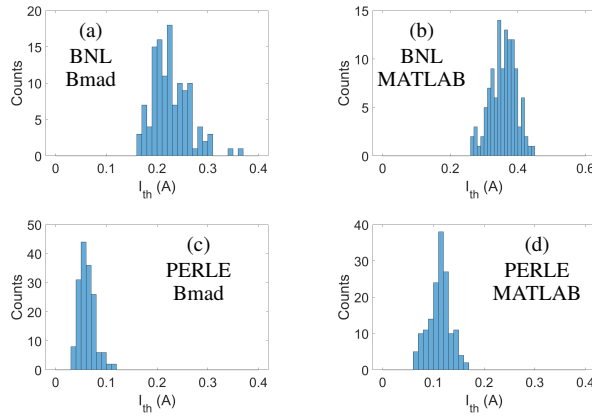


Figure 4: Threshold current scan results of two types of cavities with two BBU programs.

HOM frequencies vary among different cavities due to manufacturing errors, leading to a frequency spread. This spread typically spans several MHz and follows a Gaussian distribution. To simulate this frequency variation, relative RMS frequency jitters of  $\sigma_f/f = 10^{-3}$  were introduced to the HOM frequencies. The results are presented in Fig. 4.

Although the two codes exhibit some discrepancies, both demonstrate that the BNL-type cavities are much more stable and possess significantly higher threshold currents than the PERLE-type. Both simulations predict that the BNL-type cavities can meet the cooler's operating current requirement of 98.5 mA. However, both codes conclusively show that the PERLE-type cavities cannot fulfill this requirement. The discrepancy between the MATLAB and Bmad tracking results is currently under investigation.

The dominant cavities and modes identified by the MATLAB BBU code are presented in Fig. 5. The 1773 MHz cavities are the most dominant, followed by the 591 MHz cavities, as expected from the figure of merit  $\xi$ . None of the 197 MHz cavities were dominant. This finding suggests the possibility of using a hybrid approach: employing one BNL-type cavity per cryomodule at higher frequencies, while using multiple PERLE-type cavities per cryomodule at lower frequencies. Given that the 197 MHz cavities are three times larger than the 591 MHz cavities and nine times larger than the 1773 MHz cavities, this hybrid approach would leverage the BBU stability of BNL-type cavities at high frequencies and the compactness of PERLE-type cavities at low frequencies.

In both cavity types, the most dominant modes are horizontal, with the highest figure of merit  $\xi$ , as expected. Although the BNL-type cavities' highest  $\xi$  values are for vertical modes (modes No. 1 and 2), they are not the most dominant overall. This indicates that particular attention should be paid to damping horizontally polarized modes.

## CONCLUSION

We compared the BBU instability performance of BNL and PERLE-type cavities. Although the frequency scaling

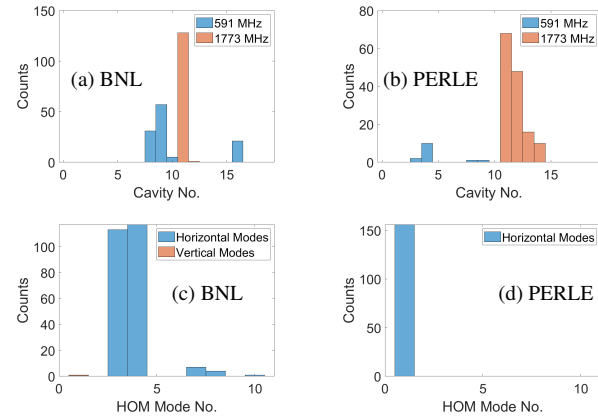


Figure 5: Dominant cavity and HOMs. (a) and (b) show which cavities set threshold currents. (c) and (d) show which modes set threshold currents.

method used for HOM parameters prevents precise threshold current estimation, it still provides a qualitative comparison of the two cavity types and a rough estimate of the threshold current. Our results show that BNL-type cavities are more stable and have significantly higher threshold currents, meeting the ERL cooler requirements, whereas PERLE-type cavities yield threshold currents below the required level. While it's not practical to use PERLE-type cavities for all three frequencies, they could still be utilized for the lower-frequency cavities since their HOM figures of merit are much lower than those of the 1773 MHz cavities, making them less dominant. We'll investigate a hybrid approach in future studies, where BNL-type cavities are used for higher frequencies and PERLE-type for lower frequencies. This approach would save space while maintaining BBU performance. Other methods under consideration to increase BBU thresholds, if necessary, are the implementation of an emittance exchange system or a BBU feedback system. It should be noted that the HOM parameters employed in this study are preliminary estimations, and consequently, the results presented herein are tentative as well. The primary objective of this work is to develop a comprehensive framework ("deck") to facilitate multiple iterations of studies with varying HOM impedance inputs in the future. This iterative methodology is intended to provide robust guidelines for establishing HOM impedance specifications pertinent to cavity design and acceptance testing.

## ACKNOWLEDGEMENTS

This work is supported by Jefferson Science Associates, LLC under U.S. DOE Contract DE-AC05-06OR23177 and Brookhaven Science Associates, LLC, Contract DESC0012704, while Xelera was supported by the U.S. DOE Small Business Innovation Research (SBIR) Phase II program under Federal Grant Number DE-SC0020514 during earlier stages of this work.

## REFERENCES

[1] R. Abdul Khalek *et al.*, “Snowmass 2021 White Paper: Electron Ion Collider for High Energy Physic”, *arXiv*, preprint arXiv:2203.13199, 2022.

[2] F. Willeke, “Electron Ion Collider Conceptual Design Report 2021”, Brookhaven Natl. Lab., USA, Rep. BNL-221006-2021-FORE.

[3] V. N. Litvinenko and Y. S. Derbenev, “Coherent electron cooling”, *Phys. Rev. Lett.*, vol. 102, p. 114801, 2009. doi:10.1103/PhysRevLett.102.114801

[4] E. Wang *et al.*, “Electron Ion Collider Strong Hadron Cooling Injector and ERL”, in *Proc. LINAC’22*, Liverpool, UK, Aug.-Sep. 2022, pp. 7-12. doi:10.18429/JACoW-LINAC2022-M02AA04

[5] O. Brüning, A. Seryi, and S. Verdú-Andrés, “Electron-Hadron Colliders: EIC, LHeC and FCC-eh”, *Front. Phys.*, vol. 10, p. 886473, 2022. doi:10.3389/fphy.2022.886473

[6] C. Gulliford *et al.*, “Design and optimization of an ERL for cooling EIC hadron beams”, in *Proc. IPAC’23*, Venice, Italy, May 2023, pp. 73–76. doi:10.18429/JACoW-IPAC2023-MOPA016

[7] K. Deitrick *et al.*, “Development of an ERL for coherent electron cooling at the Electron-Ion Collider”, presented at IPAC’24, Nashville, Tennessee, USA, May 2024, this conference.

[8] W. Xu *et al.*, “Evaluation of baseline 5-cell cavity for EIC RCS, HSR and SHC ERL”, BNL, Upton, NY, United States, Rep. BNL-224465-2023-TECH; EIC-ADD-TN-060; TRN: US2403709.

[9] R. A. Rimmer *et al.*, “Cavity and cryomodule developments for EIC”, in *Proc. eeFACT’22*, Frascati, Italy, Oct. 2022. doi:10.18429/JACoW-eeFACT2022-WEXAS0101

[10] M. Klein and A. Stocchi, “PERLE: A high power energy recovery facility for Europe a contribution to the update of the European strategy on particle physics”, CERN, Geneva, Switzerland, Rep. LHeC-Note-003-2018.

[11] S. A. Bogacz *et al.*, “Beam dynamics driven design of powerful energy recovery linac for experiments”, *Phys. Rev. Accel. Beams*, vol. 27, p. 031603, 2024. doi:10.1103/PhysRevAccelBeams.27.031603

[12] O. Brunner *et al.*, “Assessment of the basic parameters of the CERN superconducting proton linac”, *Phys. Rev. ST Accel. Beams*, vol. 12, p. 070402, 2009. doi:10.1103/PhysRevSTAB.12.070402

[13] N. Valles, “Pushing the frontiers of superconducting radio frequency science: from the temperature dependence of the superheating field of niobium to higher-order mode damping in very high quality factor accelerating structures”, Ph.D. Thesis, Cornell Univ., Ithaca, NY, USA, 2014.

[14] W. Lou and G. H. Hoffstaetter, “Beam breakup current limit in multiturn energy recovery linear accelerators”, *Phys. Rev. Accel. Beams*, vol. 22, p. 112801, 2019. doi:10.1103/PhysRevAccelBeams.22.112801